Anharmonic effects in light scattering due to optical phonons in silicon

M. Balkanski, R. F. Wallis,* and E. Haro
Laboratoire de Physique des Solides, associé au Centre National de la Recherche Scientifique, Université Pierre et Marie Curie, Tour 13, Deuxième Etage, 4 Place Jussieu, F-75230 Paris Cedex 05, France
(Received 13 July 1982; revised manuscript received 21 April 1983)

Systematic measurements by light scattering of the linewidth and frequency shift of the $\vec{q}=0$ optical phonon in silicon over the temperature range of 5–1400 K are presented. Both the linewidth and frequency shift exhibit a quadratic dependence on temperature at high temperatures. This indicates the necessity of including terms in the phonon proper self-energy corresponding to four-phonon anharmonic processes.

I. INTRODUCTION

Experimental studies of the inelastic scattering of light by crystals have provided a great deal of information concerning the optical modes of vibration at the center of the Brillouin zone. In pure materials one finds typically that both the line center and the linewidth vary with temperature. This temperature dependence can be attributed to the anharmonic terms in the vibrational potential energy.[1]

If one restricts oneself to cubic anharmonicity in second order, the damping constant which characterizes the linewidth is proportional to the absolute temperature T in the high-temperature limit, but when one includes quartic anharmonicity to second order and/or cubic anharmonicity to fourth order, the damping constant involves terms proportional to T^2 in the high-temperature limit.[2] For the case of silicon, Hart, Aggarwal, and Lax[3] have measured the frequency shift of the line center and the damping constant over a range of temperatures from 20 to 770 K. They found that their data for the frequency shift agree rather well with the theoretical calculations of Cowley[4] based on cubic anharmonicity to second order, but their data for the damping constant show significant deviations from Cowley's results. Hart *et al.* were able to show, however, that their data for the damping constant can be fitted satisfactorily by the cubic anharmonic model of Klemens[5] if the zero-temperature value of the damping constant is properly chosen.

Recently, Tsu and Hernandez[6] have reported measurements of the frequency shifts of both one-phonon and two-phonon Raman lines for silicon over the temperature range 20–900 °C. Where their results overlap with those of Hart *et al.*, the agreement is good. No data on the linewidth is presented by Tsu and Hernandez.

In the present paper, measurements of the light scattering spectrum of silicon are reported for the temperature range between 5 and 1400 K. The temperature dependences of the frequency shift and damping constant of the Raman active LO phonon are analyzed in terms of cubic and quartic anharmonic contributions. It is found that at the higher temperatures, cubic anharmonic terms to second order are not sufficient to fit the data, but the inclusion of higher-order terms involving cubic and/or quartic anharmonicity makes possible a satisfactory fit.

II. ANHARMONICITY IN LIGHT SCATTERING BY OPTICAL PHONONS

For a system whose equilibrium atomic positions are specified by

$$\vec{R}^{(0)}(l,\kappa)=\vec{R}(l)+\vec{R}(\kappa)\ , \tag{2.1}$$

where $\vec{R}(l)=l_1\vec{\tau}_1+l_2\vec{\tau}_2+l_3\vec{\tau}_3$, the $\vec{\tau}_i$ are primitive translation vectors, the l_i are integers, and $\vec{R}(\kappa)$ is a vector of the basis; the vibrational Hamiltonian can be written as

$$\begin{aligned}H=&\tfrac{1}{2}\sum_{l,\kappa,\alpha}\frac{1}{M_\kappa}P_\alpha^2(l,\kappa)+\tfrac{1}{2}\sum_{l,\kappa,\alpha}\sum_{l',\kappa',\beta}\Phi_{\alpha\beta}(l,\kappa;l',\kappa')u_\alpha(l,\kappa)u_\beta(l',\kappa')\\&+\tfrac{1}{6}\sum_{l,\kappa,\alpha}\sum_{l',\kappa',\beta}\sum_{l'',\kappa'',\gamma}\Phi_{\alpha\beta\gamma}(l,\kappa;l',\kappa';l'',\kappa'')u_\alpha(l,\kappa)u_\beta(l',\kappa')u_\gamma(l'',\kappa'')\\&+\tfrac{1}{24}\sum_{l,\kappa,\alpha}\sum_{l',\kappa',\beta}\sum_{l'',\kappa'',\gamma}\sum_{l''',\kappa''',\delta}\Phi_{\alpha\beta\gamma\delta}(l,\kappa;l',\kappa';l'',\kappa'';l''',\kappa''')u_\alpha(l,\kappa)u_\beta(l',\kappa')u_\gamma(l'',\kappa'')u_\delta(l''',\kappa''')+\cdots\ ,\end{aligned} \tag{2.2}$$

where $\vec{u}(l,\kappa)$ is the displacement of atom l,κ from its equilibrium position and $\Phi_{\alpha\beta}$, $\Phi_{\alpha\beta\gamma}$, and $\Phi_{\alpha\beta\gamma\delta}$ are the harmonic, cubic anharmonic, and quartic anharmonic force constants, respectively. The first two terms are the harmonic Hamiltonian H_0. The remaining terms are the anharmonic Hamiltonian H_A. We diagonalize the harmonic Hamiltonian by means of the normal-coordinate transformation

$$\vec{u}(l,\kappa)=\left[\frac{\hbar}{2M_\kappa N}\right]^{1/2}\sum_{\vec{q},j}\frac{\vec{W}(\kappa\,|\,\vec{q},j)}{(\omega_{\vec{q},j})^{1/2}}e^{i\vec{q}\cdot\vec{R}(l)}A_{\vec{q},j}\ , \tag{2.3}$$

 ©1983 The American Physical Society

$$\vec{P}(l,\kappa)=-i\left[\frac{\hbar M_\kappa}{2N}\right]^{1/2}\sum_{\vec{q},j}(\omega_{\vec{q},j})^{1/2}\vec{W}(\kappa\mid\vec{q},j)\times e^{i\vec{q}\cdot\vec{R}(l)}B_{\vec{q},j}\ . \tag{2.4}$$

Here $\omega_{\vec{q},j}$ is the normal-mode frequency for wave vector $\vec{q}$ and branch index j, $\vec{W}(\kappa\mid\vec{q},j)$ is the polarization vector for the normal mode, M_κ is the mass of an atom of type κ, and N is the number of unit cells in the crystal. The field operators $A_{\vec{q},j}$ and $B_{\vec{q},j}$ are specified in terms of the phonon creation and annihilation operators $b^\dagger_{\vec{q},j}$ and $b_{\vec{q},j}$ by the relations

$$A_{\vec{q},j}=b_{\vec{q},j}+b^\dagger_{-\vec{q},j}\ , \tag{2.5}$$

$$B_{\vec{q},j}=b_{\vec{q},j}-b^\dagger_{-\vec{q},j}\ . \tag{2.6}$$

After making the normal-coordinate transformation, the contributions to the Hamiltonian take the forms

$$H_0=\tfrac{1}{4}\sum_{\vec{q},j}\hbar\omega_{\vec{q},j}(A^\dagger_{\vec{q},j}A_{\vec{q},j}+B^\dagger_{\vec{q},j}B_{\vec{q},j})=\sum_{\vec{q},j}\hbar\omega_{\vec{q},j}(b^\dagger_{\vec{q},j}b_{\vec{q},j}+\tfrac{1}{2})\ , \tag{2.7}$$

$$H_A=\sum_{\vec{q},j;\vec{q}',j';\vec{q}'',j''}V(\vec{q},j;\vec{q}',j';\vec{q}'',j'')A_{\vec{q},j}A_{\vec{q}',j'}A_{\vec{q}'',j''}+\sum_{\vec{q},j,\ldots,\vec{q}''',j'''}V(\vec{q},j;\vec{q}',j';\vec{q}'',j'';\vec{q}''',j''')A_{\vec{q},j}A_{\vec{q}',j'}A_{\vec{q}'',j''}A_{\vec{q}''',j'''}+\cdots\ . \tag{2.8}$$

The anharmonic coefficients V are given by

$$V(\vec{q},j;\vec{q}',j';\vec{q}''j'')=\frac{1}{6}\left[\frac{\hbar}{2N}\right]^{3/2}(\omega_{\vec{q},j}\omega_{\vec{q}',j'}\omega_{\vec{q}'',j''})^{-1/2}N\Delta(\vec{q}+\vec{q}'+\vec{q}'')\times\sum_{\kappa,\alpha}\sum_{\bar{l}',\kappa',\beta}\sum_{\bar{l}'',\kappa'',\gamma}\Phi_{\alpha\beta\gamma}(0,\kappa;\bar{l}',\kappa';\bar{l}'',\kappa'')\times\frac{W_\alpha(\kappa\mid\vec{q},j)W_\beta(\kappa'\mid\vec{q}';j')W_\gamma(\kappa''\mid\vec{q}'',j'')}{(M_\kappa M_{\kappa'}M_{\kappa''})^{1/2}}e^{i[\vec{q}'\cdot\vec{R}(\bar{l}')+\vec{q}''\cdot\vec{R}(\bar{l}'')]}\ , \tag{2.9}$$

$$V(\vec{q},j;\vec{q}',j';\vec{q}'',j'';\vec{q}'''j''')=\frac{1}{24}\left[\frac{\hbar}{2N}\right]^{2}(\omega_{\vec{q},j}\cdots\omega_{\vec{q}''',j'''})^{-1/2}N\Delta(\vec{q}+\vec{q}'+\vec{q}''+\vec{q}''')\times\sum_{\kappa,\alpha}\sum_{\bar{l}',\kappa',\beta}\cdots\sum_{\bar{l}''',\kappa''',\delta}\Phi_{\alpha\beta\gamma\delta}(0,\kappa;\bar{l}',\kappa';\bar{l}'',\kappa'';\bar{l}''',\kappa''')\times\frac{W_\alpha(\kappa\mid\vec{q},j)W_\beta(\kappa'\mid\vec{q}',j')W_\gamma(\kappa''\mid\vec{q}'',j'')W_\delta(\kappa'''\mid\vec{q}''',j''')}{(M_\kappa\cdots M_{\kappa'''})^{1/2}}\times e^{i[\vec{q}\cdot\vec{R}(\bar{l}')+\vec{q}''\cdot\vec{R}(\bar{l}'')+\vec{q}'''\cdot\vec{R}(\bar{l}''')]}\ , \tag{2.9}$$

where

$$\Delta(\vec{q})=\begin{cases}1 & \text{if } \vec{q}=\vec{G}\\ 0 & \text{otherwise}\end{cases} \tag{2.10}$$

and $\vec{G}$ is a vector of the reciprocal lattice.

In the case of light scattering, the efficiency for Stokes scattering by zone-center LO phonons in a homopolar crystal is given[7] by

$$\frac{d^2S}{d\omega\,d\Omega}=\frac{e^4LV}{2\pi\hbar^3m^4a^2MNc^4\omega_{\vec{0},j}}\left[\frac{\omega_S}{\omega_I}\right]\times(n_0+1)\,|\,R(j;I,S)\,|^2\times\frac{\Gamma(\vec{0},j;\omega)}{[\omega-\Omega(\vec{0},j;\omega)]^2+\Gamma^2(\vec{0},j;\omega)}\ , \tag{2.11}$$

where $R(j;I,S)$ is the Raman tensor, the branch index j refers to the longitudinal optical branch, $\vec{\eta}_I$ ($\vec{\eta}_S$) is the wave vector of the incident (scattered) radiation, a is the lattice constant, L is the crystal thickness, $\omega_{\vec{0},j}$ is the zone-center LO-phonon frequency, and n_0 is the mean number of LO phonons.

The resonant frequency $\Omega(\vec{0},j;\omega)$ in Eq. (2.11) determines the scattering line position and is given to first approximation by

$$\Omega(\vec{0},j;\omega)=\omega_{\vec{0},j}+\Delta(\vec{0},j;\omega)\ . \tag{2.12}$$

The quantities $\Delta(\vec{0},j;\omega)$ and $\Gamma(\vec{0},j;\omega)$ specify the real and imaginary parts of the proper self-energy, $P(\vec{0},j;\omega)$, according to the relation[1]

$$\lim_{\epsilon\to0^+}P(\vec{0},j;\omega+i\epsilon)=-\beta\hbar[\Delta(\vec{0},j;\omega)-i\Gamma(\vec{0},j;\omega)] \tag{2.13}$$

and are referred to as the frequency shift and damping constant, respectively. Each of these quantities is the sum of contributions arising from the cubic, quartic, and higher-order terms in the anharmonic Hamiltonian H_A. The cubic and quartic contributions up to and including second-order terms are given by[1]

$$\Delta^{(3)}(\vec{0},j;\omega)=-\frac{18}{\hbar^2}\sum_{\vec{q}_1,j_1}\sum_{\vec{q}_2,j_2}|V(\vec{0},j;\vec{q}_1,j_1;\vec{q}_2,j_2)|^2 \times\mathscr{P}\left[\frac{n_1+n_2+1}{\omega+\omega_1+\omega_2}-\frac{n_1+n_2+1}{\omega-\omega_1-\omega_2}+\frac{n_1-n_2}{\omega-\omega_1+\omega_2}-\frac{n_1-n_2}{\omega+\omega_1-\omega_2}\right], \tag{2.14a}$$

$$\Delta^{(4a)}(\vec{0},j;\omega)=\frac{24}{\hbar}\sum_{\vec{q}_1,j_1}V(\vec{0},j;\vec{0},j;\vec{q}_1,j_1;-\vec{q}_1,j_1)(n_1+\tfrac{1}{2}), \tag{2.14b}$$

$$\begin{aligned}\Delta^{(4b)}(\vec{0},j;\omega)=-\frac{96}{\hbar^2}\sum_{\vec{q}_1,j_1}\sum_{\vec{q}_2,j_2}\sum_{\vec{q}_3,j_3}|V(\vec{0},j;\vec{q}_1,j_1;\vec{q}_2,j_2;\vec{q}_3,j_3)|^2 \\ \times\mathscr{P}\Big\{[(n_1+1)(n_2+1)(n_3+1)-n_1n_2n_3] \\ \times\left[\frac{1}{\omega+\omega_1+\omega_2+\omega_3}-\frac{1}{\omega-\omega_1-\omega_2-\omega_3}\right] \\ +3[n_1(n_2+1)(n_3+1)-(n_1+1)n_2n_3] \\ \times\left[\frac{1}{\omega-\omega_1+\omega_2+\omega_3}-\frac{1}{\omega+\omega_1-\omega_2-\omega_3}\right]\Big\},\end{aligned} \tag{2.14c}$$

$$\Delta^{(4c)}(\vec{0},j;\omega)=-\frac{576}{\hbar^2}\sum_{\vec{q}_1,j_1}\sum_{j_2}\sum_{\vec{q}_3,j_3}V(\vec{0},j;\vec{0},j;-\vec{q}_1,j_1;\vec{q}_1,j_2)V(\vec{q}_1,j_1;-\vec{q}_1,j_2;\vec{q}_3;j_3;-\vec{q}_3,j_3) \times\mathscr{P}\left[\frac{n_1+n_2+1}{\omega_1+\omega_2}-\frac{n_1-n_2}{\omega_1-\omega_2}\right](n_3+\tfrac{1}{2}), \tag{2.14d}$$

$$\Gamma^{(3)}(\vec{0},j;\omega)=\frac{18\pi}{\hbar^2}\sum_{\vec{q}_1,j_1}\sum_{\vec{q}_2,j_2}|V(\vec{0},j;\vec{q}_1,j_1;\vec{q}_2,j_2)|^2 \times\{(n_1+n_2+1)[\delta(\omega-\omega_1-\omega_2)-\delta(\omega+\omega_1+\omega_2)] +(n_1-n_2)[\delta(\omega+\omega_1-\omega_2)-\delta(\omega-\omega_1+\omega_2)]\}, \tag{2.15a}$$

$$\begin{aligned}\Gamma^{(4)}(\vec{0},j;\omega)=\frac{96\pi}{\hbar^2}\sum_{\vec{q}_1,j_1}\sum_{\vec{q}_2,j_2}\sum_{\vec{q}_3,j_3}|V(\vec{0},j;\vec{q}_1,j_1;\vec{q}_2,j_2;\vec{q}_3,j_3)|^2 \\ \times\{[(n_1+1)(n_2+1)(n_3+1)-n_1n_2n_3][\delta(\omega-\omega_1-\omega_2-\omega_3)-\delta(\omega+\omega_1+\omega_2+\omega_3)] \\ +3[n_1(n_2+1)(n_3+1)-(n_1+1)n_2n_3] \\ \times[\delta(\omega+\omega_1-\omega_2-\omega_3)-\delta(\omega-\omega_1+\omega_2+\omega_3)]\},\end{aligned} \tag{2.15b}$$

where $\mathcal{P}$ denotes the principal value. In Eqs. (2.14) and (2.15) we have written

$$\omega_i = \omega_{\vec{q}_i,j_i}\ , \quad i=1,2,3 \tag{2.16a}$$

$$n_i \equiv n_{\vec{q}_i,j_i} = \frac{1}{e^{\beta\hbar\omega_{\vec{q}_i,j_i}}-1}\ , \quad i=1,2,3 \tag{2.16b}$$

where $\beta = 1/k_B T$. The various contributions to the frequency shift and damping constant are shown diagrammatically in Fig. 1. In addition, there are other diagrams not shown in Fig. 1 which can give nonzero contributions due to the fact that the atoms in silicon do not lie at centers of inversion symmetry.

A specific remark should be made about the temperature behavior of Δ and Γ. At high temperatures, i.e., temperatures larger than the Debye temperature, the cubic anharmonic terms in Δ and Γ given by Eqs. (2.14a) and (2.15a), respectively, vary linearly with T. The quartic anharmonic term in Δ corresponding to Eq. (2.14b) also varies linearly with T, but the quadratic terms corresponding to Eqs. (2.14c) and (2.14d) vary quadratically with T. The quartic anharmonic term in Γ corresponding to Eq. (2.15b) also varies quadratically with T. Additional T^2 contributions to both Δ and Γ arise from terms corresponding to the diagrams in Fig. 2.

The light scattering process can be viewed as involving the absorption of a photon $\hbar\omega_I$, the emission of a photon $\hbar\omega_S$, and the creation of an optical phonon $0j$ which then decays via anharmonicity into two phonons, three phonons, etc. The production of two and three phonons is shown diagrammatically in Figs. 3(a) and 3(c). At nonzero temperatures, processes can also occur in which the decay of the optical phonon $0j$ is accompanied by the absorption of another phonon, and the emission of one or more phonons, as shown in Figs. 3(b) and 3(d) for the cases of one and two emitted phonons, respectively.

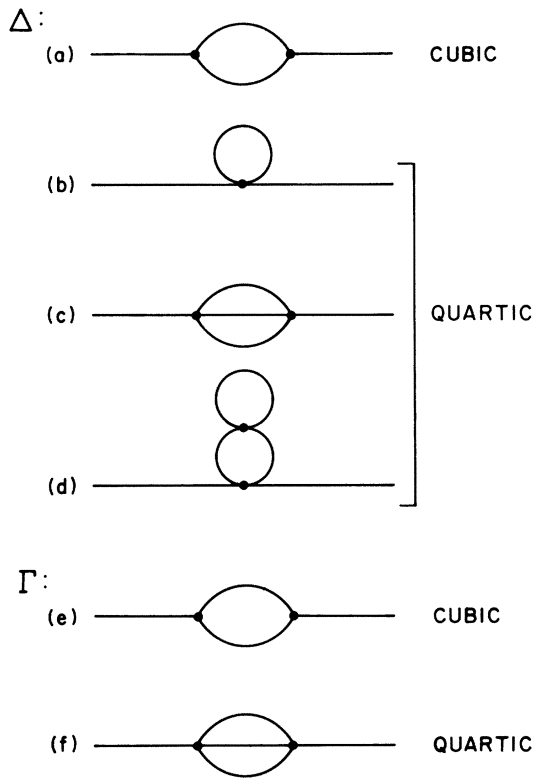

FIG. 1. Diagrams representing contributions to the frequency shift Δ and damping constant Γ for the Raman-active LO mode in silicon.

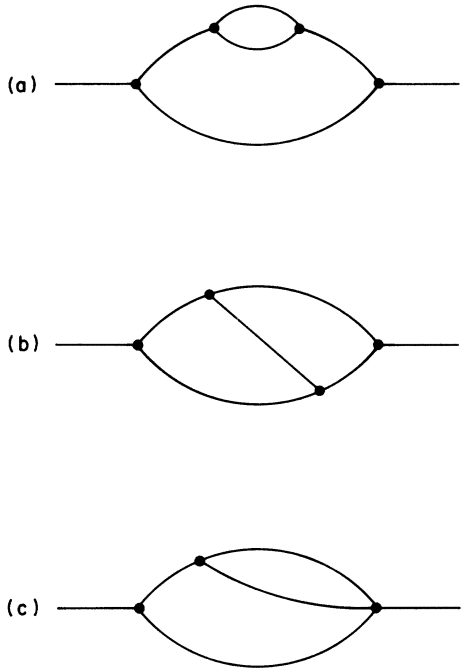

FIG. 2. Diagrams representing higher-order contributions to the proper self-energy of the Raman-active LO mode in silicon.

III. EXPERIMENTAL RESULTS

Light scattering measurements have been performed with a CODERG PHO spectrometer and an excitation laser on single crystal nondoped silicon with a resistivity of 100 Ω cm and oriented with a (111) face perpendicular to the incident beam. In view of the large temperature range explored the temperature was regulated in a liquid-He cryostat for low temperatures, an electrically heated furnace for the intermediate temperatures, and by laser heating at high temperatures.

The sample temperature was measured by a platinum resistor for low temperatures, by a thermocouple in the intermediate range, and by an optical pyrometer at high temperatures. Verification of the measured temperature was made by two additional methods. The first used the integrated ratio of the Stokes to anti-Stokes Raman peaks. The intensity of the Stokes and anti-Stokes peaks being proportional, respectively, to n_0+1 and n_0, the intensity ratio is

$$\frac{I_S}{I_{AS}} = \exp\left[\frac{\hbar\omega_0}{k_B T}\right], \tag{3.1}$$

where ω_0 is the Raman frequency. (We omit the subscript j from here on.)

The second method was based on the black-body radiation of the sample. If we admit that the sample is a black body we can apply Planck's law for the power emitted per

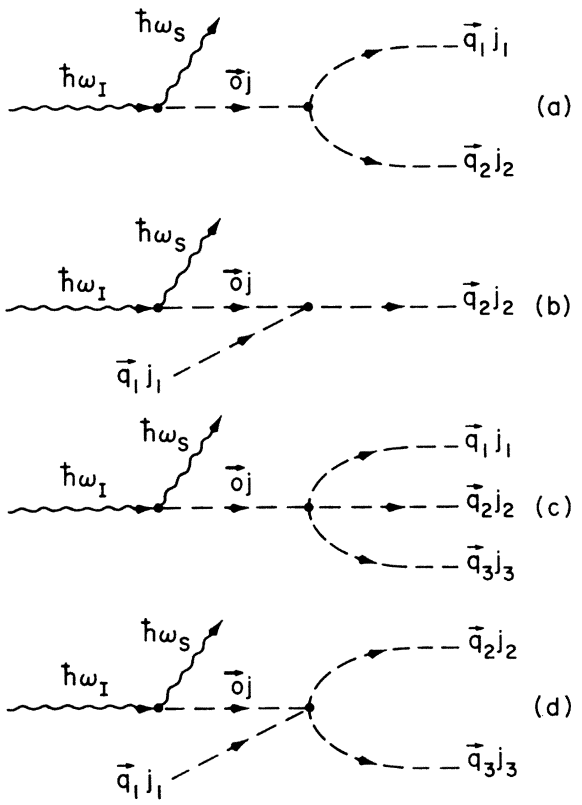

FIG. 3. Diagrams representing three- and four-phonon anharmonic processes contributing to the decay of the Raman-active LO mode in silicon.

unit area,

$$P_e(\omega)d\omega = a(\omega)\frac{\hbar}{4\pi^2c^2}\frac{\omega^3}{e^{\hbar\omega/k_BT}-1}d\omega\ , \tag{3.2}$$

and with $a(\omega)=1$ get the sample temperature.

The shape and the position of the peak due to scattering by the Raman-active LO mode in silicon vary for different temperatures. In Fig. 4 we show for comparison two spectra taken at 295 and 1140 K. From these spectra we can deduce the values of Γ and Ω for these two temperatures: for $T=295$ K, $\Gamma(0,\mathrm{LO})=4$ cm^{-1}, and $\Omega(0,\mathrm{LO})=520$ cm^{-1} and for $T=1140$ K, $\Gamma(0,\mathrm{LO})=14$ cm^{-1} and

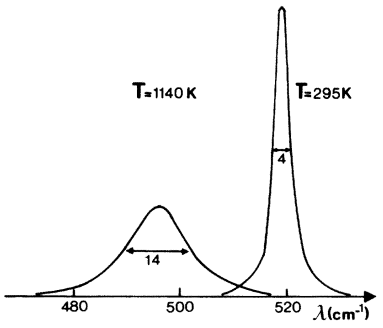

FIG. 4. First-order Raman spectra for silicon at 295 and 1140 K. The line position of the zone-center LO mode shifts from 520 cm^{-1} at 295 K to 498 cm^{-1} at 1140 K and the linewidth from 4 cm^{-1} at 295 K to 14 cm^{-1} at 1140 K.

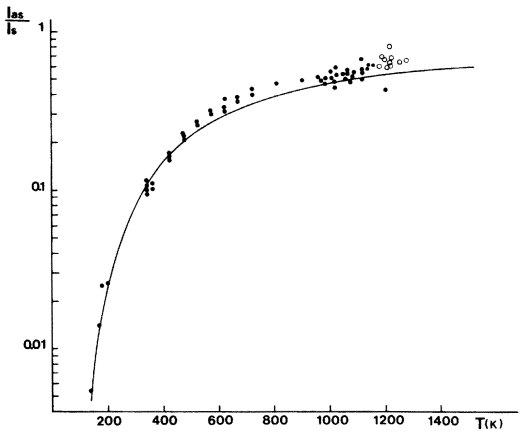

FIG. 5. Anti-Stokes to Stokes intensity ratio vs temperature, considering the correction as discussed in the text. The closed circles represent points for which temperature was measured by a Pt resistor, a thermocouple and for temperatures above 600° C by an optical pyrometer. The open circles are points obtained by heating the sample with the laser and the oven; their temperature is not precisely determined. The theoretical curve $\exp(-\hbar\omega_0/k_BT)$ is represented by a solid line.

$\Omega(0,\mathrm{LO})=498$ cm^{-1}. The Stokes to anti-Stokes ratio of the intensity of these peaks gives the temperature by using the solid line representation given in Fig. 5. In this figure the black circles represent the Pt resistor, thermocouple, and pyrometric measurements of the temperature. In order to reach the melting point, we heated the sample with the oven and the laser, by increasing the power beam. This is represented by the circles. We should note that for these points we were unable to measure the temperature accurately. The calibration of the solid line applies after the measured Raman intensities have been corrected for the actual absorption coefficient and the frequency dependence of the Raman efficiency. In applying these corrections the expression for the intensity ratio becomes

$$\frac{I_S}{I_{\mathrm{AS}}}=\frac{\alpha_I+\alpha_{\mathrm{AS}}}{\alpha_I+\alpha_S}\left[\frac{\omega_S}{\omega_{\mathrm{AS}}}\right]^3\frac{S(\omega_I,\omega_S)}{S(\omega_I,\omega_{\mathrm{AS}})}\exp\left[\frac{\hbar\omega_0}{k_BT}\right]\ , \tag{3.3}$$

where $\alpha_I,\alpha_{\mathrm{AS}},\alpha_S$ are the absorption constants at the frequencies $\omega_I,\omega_{\mathrm{AS}},\omega_S$ (incident beam, anti-Stokes, and Stokes) and $S(\omega_I,\omega_S)$ and $S(\omega_I,\omega_{\mathrm{AS}})$ are the Raman cross sections at the involved frequencies. Practically all the points obtained by pyrometric measurements are above the curve given by the Raman intensity ratio. This indicates that the temperature determined by this method is systematically higher than that obtained by other measurements. A better knowledge of the correction factors is therefore necessary in order for this method to be used for temperature measurements.

The damping constant and the frequency shift have been investigated systematically as a function of temperature. Figure 6 gives the temperature variation of the damping constant $\Gamma(T)$ between 5 and 1400 K. The dashed curve represents $\Gamma(T)$ calculated from the relation[3]

$$\Gamma(T)=\Gamma(0)\left[1+\frac{2}{e^x-1}\right]\ , \tag{3.4}$$

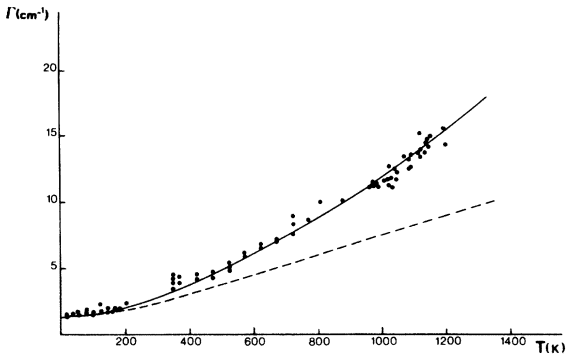

FIG. 6. Temperature dependence of the damping constant Γ for the Raman-active LO mode in silicon. The solid curve gives the theoretical fit using both three- and four-phonon processes. The dashed curve gives the theoretical fit using only three-phonon processes. The open and closed circles have the same significance as in Fig. 5.

where $x=\hbar\omega_0/2k_BT$ and $\Gamma(0)=1.40$ cm^{-1}. Equation (3.4) is an approximate expression for the temperature dependence of the damping constant based on three-phonon processes (cubic anharmonicity in second order) and the simple Klemens[5] model. It seriously underestimates the damping constant at high temperatures. We attribute this discrepancy at least in part to the neglect of four-phonon processes associated with the diagrams in Figs. 1(f) and 2(a)–2(c).

It is of interest to investigate whether this discrepancy can be eliminated by generalizing Eq. (3.4) to include the contribution of four-phonon processes. Following the approach of Klemens[5] we write the kinetic equation for the net rate of decay of an incident phonon into three thermal phonons in the form

$$\frac{d}{dt}(\delta n_0)=-B[(\delta n_0+n_0)(n_1+1)(n_2+1)(n_3+1) -(\delta n_0+n_0+1)n_1n_2n_3], \tag{3.5}$$

where δn_0 is the deviation of the incident phonon occupation number from its thermal equilibrium value n_0 and B is a constant. Using the equilibrium condition

$$n_0(n_1+1)(n_2+1)(n_3+1)-(n_0+1)n_1n_2n_3=0, \tag{3.6}$$

we can rewrite Eq. (3.5) as

$$\frac{d}{dt}(\delta n_0)=-B(n_1n_2+n_1n_3+n_2n_3+n_1+n_2 +n_3+1)\delta n_0 . \tag{3.7}$$

Energy conservation can be satisfied in the simple Klemens fashion by setting $\omega_1=\omega_2=\omega_3=\omega_0/3$. Consequently, $n_1=n_2=n_3$. The generalization of Eq. (3.4) to four-phonon processes then takes the form

$$\Gamma(T)=A\left[1+\frac{2}{e^x-1}\right]+B\left[1+\frac{3}{e^y-1}+\frac{3}{(e^y-1)^2}\right], \tag{3.8}$$

where $y=\hbar\omega_0/3k_BT$ and A and B are constants. In the high-temperature limit, the factors multiplying A and B in Eq. (3.8) vary as T and T^2, respectively.

Equation (3.8) has been used to fit the experimental data presented in Fig. 6 by suitably choosing the constants A and B. The best values of A and B are found to be 1.295 and 0.105 cm^{-1}, respectively, and the resulting plot of $\Gamma(T)$ vs T is given by the solid curve in Fig. 6. We see that the agreement between the calculated curve and the experimental points is now quite good.

The experimental results for the line position $\Omega(T)$ as a function of T are shown in Fig. 7. Also shown is the fit to the data (solid curve) specified by the expressions

$$\Omega(T)=\omega_0+\Delta(T) \tag{3.9}$$

and

$$\Delta(T)=C\left[1+\frac{2}{e^x-1}\right]+D\left[1+\frac{3}{e^y-1}+\frac{3}{(e^y-1)^2}\right], \tag{3.10}$$

where ω_0, C, and D are constants with the values 528, -2.96, and -0.174 cm^{-1}, respectively. Equation (3.10) is the analog of Eq. (3.8) and specifies the contributions of three-phonon and four-phonon processes to the frequency shift. The agreement between the experimental points and the solid curve is seen to be good.

If we try to fit the experimental data with three-phonon processes only by omitting the term in Eq. (3.10) with the factor D, we obtain the dashed curve in Fig. 7 with $\omega_0=529$ cm^{-1} and $C=-4.24$ cm^{-1}. Although this curve fits the data well at temperatures up to 600 K, it is clearly inadequate at higher temperatures. This demonstrates the necessity of including terms corresponding to four-phonon processes in the expression for $\Delta(T)$.

In principle, the four-phonon contributions in Eqs. (3.8) and (3.10) should include terms arising from difference processes of the type represented by Fig. 3(d). We have omitted such terms on the grounds that their inclusion

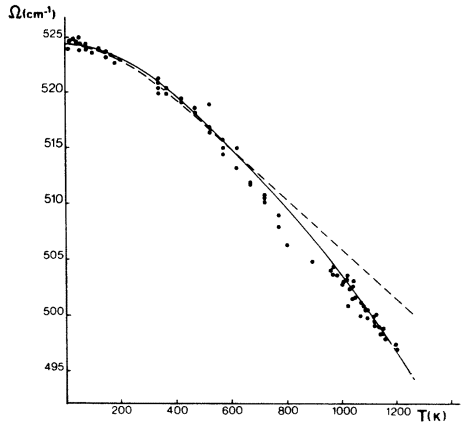

FIG. 7. Temperature dependence of the line position Ω for the Raman-active LO mode in silicon. The solid curve gives the theoretical fit using both three- and four-phonon processes. The dashed curve gives the theoretical fit using only three-phonon processes. The open and closed circles have the same significance as in Fig. 5.

would simply introduce additional terms varying as T and as T^2 in the high-temperature limit and would not add any new qualitative features.

IV. DISCUSSION

We have seen in the previous section that the extension of the Klemens-Hart-Aggarwal-Lax model[3,5] to include four-phonon processes provides a good fit to the experimental values for the frequency shift and damping constant of the Raman-active mode in silicon up to 1400 K. This fit is achieved by suitably choosing two adjustable parameters for each of the two quantities. Since one would expect the contribution of four-phonon processes to be small compared to that of three-phonon processes, the ratios B/A and D/C should be small. The actual values of these ratios are 0.08 and 0.06, respectively, so this expectation is fulfilled.

It would, of course, be desirable to carry out a first-principles calculation of the frequency shift and damping constant arising from both cubic and quartic anharmonicity. However, such a calculation is by no means trivial. The principal difficulty is that a simple model such as a nearest-neighbor model is inadequate to describe either the harmonic or the anharmonic properties of silicon. This was shown a quarter century ago by Herman[8] and by Lax[9] for the harmonic properties and very recently by Wanser and Wallis[10] for anharmonic properties. Long-range forces are necessary for a proper description and can be introduced via a shell model,[11] a bond charge model,[12] or a model containing dipole-dipole and/or quadrupole-quadrupole interactions.[9,10,13]

Cowley[4] has carried out a calculation of the frequency shift and damping constant for silicon at temperatures up to 500 K using a shell model for the harmonic forces and a nearest-neighbor model for the anharmonic forces. Reasonable agreement with the experimental data was obtained by Cowley for the frequency shifts, but not the damping constant.[3] We are currently engaged in making a calculation of these quantities using the long-range force model of Wanser and Wallis generalized to quartic anharmonicity.

ACKNOWLEDGMENTS

We wish to thank Consejo Nacional de Ciencia y Tecnología (CONACYT) of Mexico for supporting the work of one of us (E.H.), the U. S. National Science Foundation for supporting the work of another of us (R.F.W.) under Grant No. DMR-82-14214, and the European Research Office for supporting the work of another of us (M.B.) under Grant No. DAJA 37-81-C-0587. One of us (E.H.) wishes to thank J. F. Morhange for helpful discussions.

---

*Permanent address: Department of Physics, University of California, Irvine, Irvine, California 92717.

[1]R. F. Wallis, I. P. Ipatova, and A. A. Maradudin, Fiz. Tverd. Tela Leningrad 8, 1064 (1966) [Sov. Phys.—Solid State 8, 850 (1966)]; I. P. Ipatova, A. A. Maradudin, and R. F. Wallis, Phys. Rev. 155, 882 (1967).

[2]D. W. Jepsen and R. F. Wallis, Phys. Rev. 125, 1496 (1962).

[3]T. R. Hart, R. L. Aggarwal, and B. Lax, Phys. Rev. B 1, 638 (1970).

[4]R. A. Cowley, J. Phys. (Paris) 26, 659 (1965).

[5]P. G. Klemens, Phys. Rev. 148, 845 (1966).

[6]R. Tsu and J. G. Hernandez, Appl. Phys. Lett. 41, 1016 (1982).

[7]R. Loudon, Proc. R. Soc. London Ser. A 275, 218 (1963).

[8]F. Herman, J. Phys. Chem. Solids 8, 405 (1959).

[9]M. Lax, Phys. Rev. Lett. 1, 133 (1958).

[10]K. H. Wanser and R. F. Wallis, J. Phys. (Paris) Colloq. 42, C6-128 (1981).

[11]W. Cochran, Proc. R. Soc. London Ser. A 253, 260 (1959).

[12]W. Weber, Phys. Rev. B 15, 4789 (1977).

[13]M. Lax, *Symmetry Principles in Solid State and Molecular Physics* (Wiley, New York, 1974).